Journal of Applied Mechanics and Technical Physics, Vol. 49, No. 2, pp. 179–187, 2008

CONSTRAINTS ON THE "RAPID" PART OF THE PRESSURE–STRAIN RATE CORRELATIONS DERIVED FROM THE SPECTRAL PRESENTATION

S. R. Bogdanov[1] **and T. J. Jongen**[2]

UDC 532.517.4

Based on the exact spectral presentation of the "rapid" part of the pressure–strain rate correlations, semi-empirical approximations used for these correlations within the framework of the second-order closures are analyzed. Simple inequalities relating the values of the model constants, mean velocity parameters, and Reynolds tensor invariants are derived. For certain types of flows, in contrast to conditions of realizability, these inequalities allow verification of the approximations before solving differential equations. It is demonstrated that some models cannot be considered as sufficiently precise ones to describe flows with high degrees of anisotropy. In particular, the condition of non-negative determinacy of the spectral matrix is violated in a considerable region of the physically admissible range of parameters. The boundaries of this region are calculated for an irrotational three-dimensional distortion and for an arbitrary two-dimensional distortion of turbulence in channel flows. Simple constraints on model constants are obtained, which allow these violations to be avoided.

Key words: *developed turbulence, spectral methods, second-order closures, realizability conditions.*

Introduction. Studying developed anisotropic turbulence involves various ideas, beginning from the theory of fractals and the renorm-group method and ending by direct numerical simulations and semi-empirical models. Nowadays calculations are performed with the so-called first-order and second-order closures.

The first-order closures based on the concept of turbulent viscosity involve direct parametrization of the Reynolds tensor $\tau_{ij} \equiv \langle u_i u_j \rangle$ via the strain rate tensor $U_{ij} \equiv \partial U_i/\partial x_j$ ($\boldsymbol{U}$ and $\boldsymbol{u}$ are the mean and fluctuating velocities, respectively; $i, j = 1, 2, 3$). The area of application of such semi-empirical approximations, however, is rather limited: experimental data show that there are no local relations between the tensors τ_{ij} and U_{ij}.

The second-order closures are based on using the transport equations for the Reynolds stresses. The main difficulty is modeling the tensor of the pressure–strain rate correlations $\Phi_{ij} = P_{ij} + P_{ji}$ ($P_{ij} \equiv \langle p\, \partial u_i/\partial x_j \rangle$; p is the fluctuating part of pressure). The following semi-empirical model expression is most widely used for this tensor [1–4]:

$$\Phi_{ij} = -\varepsilon(C_1^0 + C_1^1 P/\varepsilon) b_{ij} + C_2 K S_{ij} + C_3 K (b_{ik} S_{kj} + S_{ik} b_{kj} - (2/3) b_{mn} S_{nm} \delta_{ij})$$

$$- C_4 K (b_{ik} W_{kj} - W_{ik} b_{kj}) + C_5 \varepsilon (b_{ik} b_{kj} - (1/3) b_{mn} b_{nm} \delta_{ij}). \qquad (1)$$

Here $S_{ij} = (U_{ij} + U_{ji})/2$ and $W_{ij} = (U_{ij} - U_{ji})/2$ are the symmetric and antisymmetric parts of the strain rate tensor, ε is the mean rate of energy dissipation, $P \equiv \tau_{ij} S_{ij} = -2K b_{ij} S_{ij}$ is the "production" of turbulence by the mean flow, $b_{ij} \equiv \tau_{ij}/(2K) - \delta_{ij}/3$ is the anisotropy tensor, K is the turbulent kinetic energy, and $\{C_i\}$ are model constants.

[1]Kareliya State Pedagogical University, Petrozavodsk 185680, Russia. [2]Unilever Research Institute, Vlaardingen 3133, the Netherlands; sbogdanov@onego.ru. Translated from Prikladnaya Mekhanika i Tekhnicheskaya Fizika, Vol. 49, No. 2, pp. 29–39, March–April, 2008. Original article submitted January 24, 2007; revision submitted April 25, 2007.

0021-8944/08/4902-0179 © 2008 Springer Science + Business Media, Inc.

Though the ideas used to construct such expressions are physically grounded, they still retain functional undeterminacy to a large extent. In particular, it is highly probable that the realizability conditions are violated; these conditions, for instance, include the inequalities [5]

$$\langle u_1^2\rangle \geqslant 0, \qquad \langle u_1 u_2\rangle^2 \leqslant \langle u_1^2\rangle\langle u_2^2\rangle \tag{2}$$

and similar inequalities that follow from the positive determinacy of the Reynolds tensor. It is difficult to predict violation of these conditions; hence, it is rather difficult to determine the boundaries of the area of applicability of this or that model expression.

At the same time, using the spectral presentation for the "rapid" part $\Phi_{ij}^{(r)}$ of the tensor of the pressure–strain rate correlations, we can obtain simple strict constraints on the values of the components of this tensor [6, 7], which, in turn, allows us to evaluate the applicability of various model expressions before cumbersome calculations are performed.

In deriving these constraints, we take into account the positive determinacy of the spectral matrix F_{ij} of the two-point correlations $R_{ij} \equiv \langle u_i(\boldsymbol{x})u_j(\boldsymbol{x}+\boldsymbol{r})\rangle$ of the fluctuating velocity:

$$F_{ij}\xi_i\bar{\xi}_j \geqslant 0 \tag{3}$$

(ξ_i is an arbitrary complex vector; the bar means complex conjugation).

Note that the realizability conditions (2), as a consequence of the positive determinacy of the Reynolds tensor, directly follow from the last inequality after its integration with respect to all possible values of the wave vector $\boldsymbol{k}$ under the condition that $\boldsymbol{\xi}$ is independent of $\boldsymbol{k}$. Choosing $U_{li}\theta_l$ as ξ_i ($\theta_l \equiv k_l/k$), more constructive inequalities can be constructed (see Sec. 1).

1. Derivation of Constraints on the Convolution $\{\boldsymbol{\Phi^{(r)}U}\}$. We use the exact presentation for the "rapid" part of the pressure–strain rate correlations (induced by the mean strain rates):

$$\Phi_{ij}^{(r)} = 2U_{lm}\int (F_{mj}\theta_l\theta_i + F_{im}\theta_l\theta_j)\,d\boldsymbol{k}. \tag{1.1}$$

The turbulence is assumed to be locally homogeneous. To make the formulas more compact, we omit the arguments $\boldsymbol{k}$ and $\boldsymbol{x}$ of the components of the spectral matrix F_{ij}, its eigenvalues and eigenvectors, and the argument $\boldsymbol{x}$ of one-point mean correlations.

Applying the convolution with respect to the subscripts i, j to the matrix U_{ji} to Eq. (1.1) and taking into account the relations $U_{ij} = S_{ij} + W_{ij}$ and $W_{ij} = -W_{ji}$, we obtain

$$\{U\Phi^{(r)}\} = 2\int F_{mi}(U_{lm}\theta_l)(U_{ji}\theta_j)\,d\boldsymbol{k} + 2\int F_{mj}(S_{lm}\theta_l)(S_{ji}\theta_i)\,d\boldsymbol{k}$$

$$- 2\int F_{mj}(W_{lm}\theta_l)(W_{ij}\theta_i)\,d\boldsymbol{k} \tag{1.2}$$

(the braces indicate the convolution of the corresponding matrices).

It should be noted that each of the three integrals in (1.2) is non-negative by virtue of the positive determinacy of the spectral matrix F_{mj}. This can be easily verified by integrating inequality (3) with the vector $S_{li}\theta_l$ or similar vectors formed with the help of the matrices U_{li} and W_{li} being used as ξ_i.

In the absence of mean rotation ($W_{ij} = 0$), there are only the first two (non-negative) terms left in the right side of Eq. (1.2), which yields the simple inequality

$$\{U\Phi^{(r)}\} \geqslant 0. \tag{1.3}$$

In the general case, where the matrix U_{ij} is not symmetric, we have also to estimate the upper limit values of integrals in relation (1.2) to derive constraints on the values of the convolution $\{U\Phi^{(r)}\}$. For this purpose, we use the presentations for the matrix F_{mj} [8]

$$F_{mj} = \overline{a_m}(\boldsymbol{k})a_j(\boldsymbol{k})\lambda_1(\boldsymbol{k}) + \overline{b_m}(\boldsymbol{k})b_j(\boldsymbol{k})\lambda_2(\boldsymbol{k}), \tag{1.4}$$

where $\boldsymbol{a}$, $\boldsymbol{b}$ and λ_1, λ_2 are the eigenvectors (normalized to unity) and the corresponding eigenvalues of this matrix; $\boldsymbol{a}^2 = \boldsymbol{b}^2 = 1$; the vectors $\boldsymbol{a}$ and $\boldsymbol{b}$ are orthogonal to the vector $\boldsymbol{\theta}$.

Obviously, $F_{ii} = \lambda_1 + \lambda_2$, and we obtain the following expression for the turbulent kinetic energy K:

$$2K \equiv \overline{u^2} \equiv \int F_{ii}\, d\boldsymbol{k} \equiv \int (\lambda_1 + \lambda_2)\, d\boldsymbol{k}. \tag{1.5}$$

With allowance for presentation (1.4), the convolution of the matrix F_{mj} with an arbitrary vector $\boldsymbol{q}$ can be presented as

$$F_{mj} q_m q_j = |\boldsymbol{qb}|^2 \lambda_1 + |\boldsymbol{qa}|^2 \lambda_2. \tag{1.6}$$

Using the inequality $|\boldsymbol{qa}|^2 \leqslant \boldsymbol{q}^2 \boldsymbol{a}^2 \equiv \boldsymbol{q}^2$ and a similar inequality for the second term in the right side of Eq. (1.6), we obtain

$$F_{mj} q_m q_j \leqslant (\lambda_1 + \lambda_2) \boldsymbol{q}^2. \tag{1.7}$$

Consecutively choosing the vectors $S_{lm}\theta_l$, $U_{lm}\theta_l$, and $W_{lm}\theta_l$ as q_m, we can easily derive constraints from above on the values of integrals in Eq. (1.2) from the last inequality. Indeed, considering, for certainty, $q_m = S_{lm}\theta_l$, we can write $\boldsymbol{q}^2$ in the form

$$\boldsymbol{q}^2 = S_{lm}^2 \theta_l \theta_m.$$

This presentation means that the value of $\boldsymbol{q}^2$ is constrained from above by the maximum value of the convolution of the matrix S_{lm}^2 (or $U_{lp}U_{mp}$ and $-W_{lm}^2$ for two other cases) with the unit vector $\boldsymbol{\theta}$. In turn, this quadratic form is constrained by the maximum eigenvalue $\|S^2\|$ of the matrix S_{lm}^2 [9]. As a result, Eq. (1.7) yields

$$F_{mj}(S_{lm}\theta_l)(S_{ji}\theta_i)\, d\boldsymbol{k} \leqslant (\lambda_1 + \lambda_2)\|S^2\|.$$

Integrating the last relation with respect to $\boldsymbol{k}$ and taking into account Eq. (1.5), we obtain

$$0 \leqslant \int F_{mj}(S_{lm}\theta_l)(S_{ji}\theta_i)\, d\boldsymbol{k} \leqslant 2K\|S^2\|. \tag{1.8}$$

As a result of similar calculations for $U_{lm}\theta_l$ and $W_{lm}\theta_l$ as $\boldsymbol{q}$ in relation (1.7), we obtain the upper estimates for $\boldsymbol{q}^2$: $\|S^2\| + \|-W^2\| - 2\|SW\|$ and $\|-W^2\|$. Then we obtain the following inequalities for the two remaining integrals in the right side of Eq. (1.2):

$$\begin{gathered} 0 \leqslant \int F_{mj}(W_{lm}\theta_l)(W_{ij}\theta_i)\, d\boldsymbol{k} \leqslant 2K\|-W^2\|, \\ 0 \leqslant \int F_{mi}(U_{lm}\theta_l)(U_{ji}\theta_j)\, d\boldsymbol{k} \leqslant 2K(\|S^2\| + \|-W^2\| - 2\|SW\|). \end{gathered} \tag{1.9}$$

Finally, substituting estimates (1.8) and (1.9) into relation (1.2), we find the sought constraints:

$$-4K\|-W^2\| \leqslant \{U\Phi^{(r)}\} \leqslant 4K(2\|S^2\| + \|-W^2\| - 2\|SW\|). \tag{1.10}$$

In contrast to the usual realizability conditions (2), the double inequality (1.10) derived from the condition of positive determinacy of the spectral matrix F_{ij} includes a model expression for the tensor $\Phi_{ij}^{(r)}$, which allows direct verification of the adequacy of these expressions. It is demonstrated in Sec. 2 that certain conclusions for particular types of flows can be made even before solving differential equations.

2. Direct Verification of the Models for $\boldsymbol{\Phi_{ij}^{(r)}}$. Relation (1.10) can be used for a preliminary analysis of applicability of all models for calculating this or that type of flows. For certainty, we consider only the simplest (linear in terms of b and U) relations (1) for $\Phi_{ij}^{(r)}$. Substituting the part of expression (1) corresponding to the "rapid" part $\Phi_{ij}^{(r)}$ of the tensor of the pressure–strain rate correlations into the main inequality (1.10) and performing some simple transformations, we obtain

$$2(2\|S^2\| + \|-W^2\| - 2\|SW\|) \geqslant C_2\{S^2\}/2 + C_3\{bS^2\} - C_4\{bWS\} \geqslant -2\|-W^2\|. \tag{2.1}$$

To simplify the calculations, we consider only two types of flows. The first one is an irrotational three-dimensional deformation including important particular cases, such as flows in diverging and converging channels. The main inequality has the simple form (1.3) or, which is equivalent, reduces to the second inequality of (2.1) with $W = 0$. The second, relatively simple type of flows is characterized by a two-dimensional matrix of the mean strain rates [10, 11]

$$\frac{\partial U_i}{\partial x_j} = (D+\omega)\delta_{i1}\delta_{j2} + (D-\omega)\delta_{i2}\delta_{j1}, \tag{2.2}$$

where D and ω are parameters characterizing plane strain and rotation. This type of flows, however, includes various flows important for practice: flow in a plane channel, plane distortion of grid turbulence, and elliptical flows. In addition, homogeneous flows of this type are of significant interest: they are usually used for "calibration" of models and for choosing the values of constants.

For flows of this type, the maximum eigenvalues $\|S^2\|$, $\|SW\|$, and $\|-W^2\|$ can be calculated directly, which yields the following estimates:

$$\|S^2\| \leqslant \{S^2\}/2, \qquad \|-W^2\| \leqslant \{-W^2\}/2, \qquad \|SW\| \leqslant (\{S^2\}\{-W^2\})^{1/2}/2. \tag{2.3}$$

With allowance for inequalities (2.3), constraint (2.1) acquires the form

$$2 + 2|R| + R^2 \geqslant C_2/2 + C_3\{bS^2\}/\{S^2\} - C_4\{bWS\}/\{S^2\} \geqslant -R^2, \tag{2.4}$$

where $R^2 \equiv -\{W^2\}/\{S^2\}$.

Following [10], we consider the convolution of the anisotropy tensor b with the matrices of the mean strain rates:

$$B_3 \equiv \{bS^2\}/\{S^2\}, \qquad B_2 \equiv \{bWS\}/\{S^2\}, \qquad B_1 \equiv \{bS\}/\{S^2\}^{1/2}. \tag{2.5}$$

With allowance for (2.5), we can write inequality (2.4) in a simple form:

$$2 + 2|R| + R^2 \geqslant C_2/2 + C_3B_3 - C_4B_2 \geqslant -R^2. \tag{2.6}$$

As the parameters $\{B_i\}$ characterizing the anisotropy tensor can take arbitrary values for the flow types considered (for instance, at the beginning of the area of distortion), the model can be treated as adequate if inequality (2.6) is satisfied in the entire range of physically possible values of $\{B_i\}$.

Let us consider the boundaries of this region in more detail. With allowance for Eqs. (2.5) and (2.2), we obtain the following relation for the invariants $\{B_i\}$:

$$B_3 = (b_{11} + b_{22})/2 \equiv -b_{33}/2, \qquad B_2 = R(b_{11} - b_{22})/2, \qquad B_1 = b_{12}\sqrt{2}. \tag{2.7}$$

Taking into account the realizability conditions (2) and writing them in the form of constraints on the anisotropy tensor components as $-1/3 \leqslant b_{ii} \leqslant 2/3$ (no summation with respect to i is performed) and $b_{12}^2 \leqslant (b_{11}+1/3)^2(b_{22}+1/3)^2$, we can determine the range of values of the invariants $\{B_i\}$ from relations (2.7).

Indeed, the first relation in (2.7) yields

$$B_3 \in [-1/3, 1/6]. \tag{2.8}$$

For a given B_3, the range of admissible values of B_2 is easily found from the second relation in (2.7):

$$B_2 \in R[-1/3 - B_3; 1/3 + B_3]. \tag{2.9}$$

Finally, for given values of B_2 and B_3, the range of the values of B_1 is determined by the inequality

$$B_1^2 \leqslant 2((B_3 + 1/3)^2 - B_2^2/R^2). \tag{2.10}$$

It should be noted that inequalities (2.8)–(2.10) for the set of the scalars $\{B_i\}$ are only a different form of recording of the usual realizability conditions (2). The admissible values of the parameters $\{B_i\}$ determined by these inequalities are plotted in Fig. 1 in the plane $(B_2/R, B_3)$. Constraints (2.8) and (2.9) are valid in the region bounded by the contour of the triangle ABC. The boundaries of this triangle are characterized by two-dimensional turbulence, the vertices A, B, and C are characterized by one-dimensional turbulence (with fluctuations along the axes 3, 2, and 1, respectively), the segments BE, CF, and AD are characterized by axisymmetric turbulence (cases $u_1^2 = u_3^2$, $u_2^2 = u_3^2$, and $u_1^2 = u_2^2$), and the point O is characterized by isotropic turbulence. Figure 1 also shows a family of hyperbolas, which are isolines of B_1 (2.10). For a given B_1, the range of possible values of the parameters B_3 and B_2/R is bounded by the corresponding hyperbola and by the segment BC.

Constraint (2.6) can be analyzed by two methods: 1) by substituting the values of the constants $\{C_i\}$ into Eq. (2.6) and by calculating the "regions of adequacy" in the plane $(B_2/R, B_3)$, i.e., finding the range of admissible values of the components of the tensor b in which constraint (2.6) is valid if appropriate models are used; 2) by

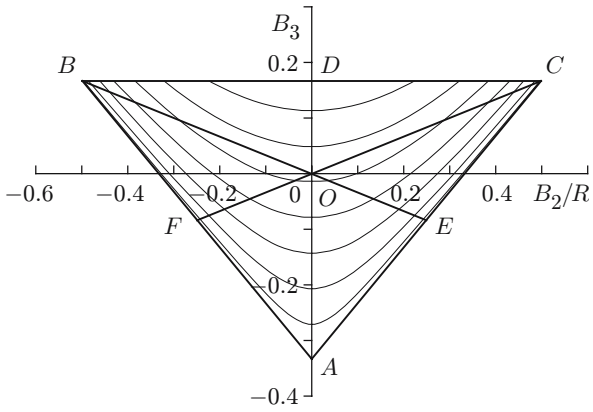

Fig. 1. Admissible values of the parameters B_3 and B_2/R: the family of hyperbolas inside the triangle ABC are the isolines of B_1.

obtaining constraints on the values of the model constants $\{C_i\}$ through substituting admissible values of the invariants B_3 and B_2 into Eq. (2.6).

Let us illustrate the second method by a simple example. In the particular case $R = 0$, relation (2.6) has the form

$$-C_2/(2C_3) \leqslant B_3 \leqslant (4 - C_2)/(2C_3). \tag{2.11}$$

Comparing inequalities (2.8) and (2.11), we obtain the following constraints on the values of the model constants:

$$4 - C_3/3 \geqslant C_2 \geqslant 2C_3/3. \tag{2.12}$$

The most famous second-order closures have the following values for the set of the constants $\{C_i\}$:

— for the Speziale–Sarkar–Gatski (SSG) model [1],

$$C_1^0 = 3.4, \quad C_1^1 = 1.8, \quad C_2 = 0.36, \quad C_3 = 1.25, \quad C_4 = 0.4, \quad C_5 = 4.2;$$

— for the Launder–Reece–Rodi (LRR) model [2],

$$C_1^0 = 3.0, \quad C_1^1 = 0, \quad C_2 = 0.8, \quad C_3 = 1.75, \quad C_4 = 1.31, \quad C_5 = 0;$$

— for the Gibson–Launder (GL) model [3],

$$C_1^0 = 3.6, \quad C_1^1 = 0, \quad C_2 = 0.8, \quad C_3 = 1.2, \quad C_4 = 1.2, \quad C_5 = 0;$$

— for the Taulbee (T) model [4],

$$C_1^0 = 3.6, \quad C_1^1 = 0, \quad C_2 = 0.8, \quad C_3 = 1.94, \quad C_4 = 1.16, \quad C_5 = 0.$$

Substituting these values into inequality (2.12) we can easily check that the left side of the inequality is valid for all models, while the right side is valid only for the GL model, and the relation $C_2 = 2C_3/3$ is satisfied exactly for the GL model.

Similarly, we consider a more general case $R \neq 0$ by using the second method. With allowance for the results obtained for the case $R = 0$, we consider only the stronger inequality (2.6):

$$C_2/2 + C_3B_3 - C_4B_2 + R^2 \geqslant 0. \tag{2.13}$$

For inequality (2.13) to be satisfied for all values of R, the discriminant of the quadratic trinomial has to be negative:

$$2(C_2 + 2C_3B_3) \geqslant C_4^2B_2^2/R^2. \tag{2.14}$$

Hence, the "dangerous" region for the model is the region where inequality (2.14) is invalid; for each particular value of B_3, the most adverse variant corresponds to the case with the maximum value of B_2, i.e., with allowance for (2.9), $B_2 = R(B_3 + 1/3)$. In this limiting case, inequality (2.14) yields the constraint

$$C_4^2B_3^2 + (2C_4^2/3 - 4C_3)B_3 + C_4^2/9 - 2C_2 \leqslant 0. \tag{2.15}$$

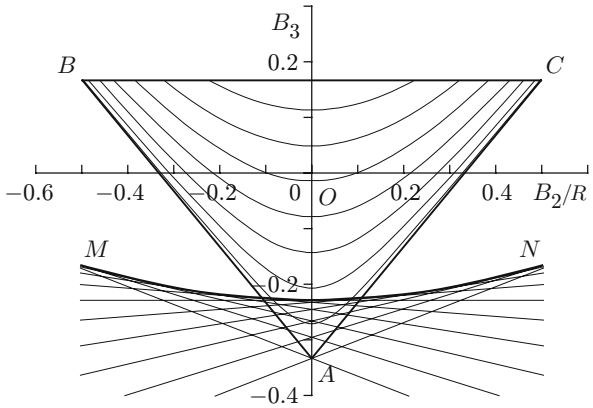

Fig. 2. "Region of adequacy" of the LRR model in calculations of elliptical flows: the region below the parabola MN is the region of violation of the realizability conditions of the model.

For constraint (2.15) to be satisfied for all values of B_3, the necessary condition is

$$C_2 \geqslant 2C_3/3 - 2C_3^2/C_4^2. \tag{2.16}$$

In addition, for condition (2.15) to be satisfied for all possible values of B_3 [see (2.8)], the minimum and maximum roots of the quadratic trinomial for B_3 in the left side of Eq. (2.15) should be smaller than $-1/3$ and greater than $1/6$, respectively. This yields the following constraints on the values of the constants:

$$C_2 \geqslant 2C_3/3; \tag{2.17}$$

$$C_3 \geqslant C_4^2/4 \quad (\text{or} \quad C_3 + 3C_2 \geqslant 3C_4^2/8 \quad \text{if} \quad C_3 \leqslant C_4^2/4). \tag{2.18}$$

Constraint (2.17), which guarantees applicability of the models near the limiting value $B_3 = -1/3$, makes inequality (2.16) stronger, but it gives no new results, as compared with the case $R = 0$ considered above. Inequalities (2.18) ensure adequacy of the models in the limiting region in the vicinity of the value $B_3 = 1/6$.

Substituting the values of the constants for various models into inequalities (2.17) and (2.18), we can easily see that inequality (2.18) is satisfied for all cases, while inequality (2.17) is satisfied for the GL model only.

If the condition $C_2 \geqslant 2C_3/3$ is violated, we can easily find the values of R at which this violation happens with the use of (2.13). Indeed, substituting the value $B_3 = -1/3$ at which this violation happens and the corresponding value $B_2 = 0$ into (2.13), we obtain

$$R \leqslant \sqrt{-(C_2 - 2C_3/3)/2}. \tag{2.19}$$

The analysis performed allows us to draw the following conclusions: 1) the necessary condition of adequacy of the models is presented in the form of inequalities (2.12), (2.17), (2.18); 2) if the inequality $C_2 \geqslant 2C_3/3$ is not satisfied, the realizability condition is violated at $R \leqslant \sqrt{-(C_2 - 2C_3/3)/2}$.

Let us analyze the constraints by using the first method, i.e., by substituting the values of the constants of each model into (2.6) and finding the range of admissible values of the parameters B_2, B_3 available for a given model. The results obtained above have a clear geometric interpretation.

Indeed, inequality (2.13) can be presented in the plane $(B_2/R, B_3)$ by a family of straight lines with R as a parameter. The envelope of this family is a parabola defined by the formula $C_2 + 2C_3B_3 = C_4^2(B_2/R)^2/2$, which agrees with (2.14). Figure 2 shows the family of these straight lines and the corresponding parabola (2.14) (for this figure, the values of the constants of the LRR model are used; the results for other models, except for the GL model, are similar). These parabolas intersect the region of admissible values of the parameters in the zone adjacent to the lower vertex of the triangle. For each value of R within the interval $[0, \sqrt{-(C_2 - 2C_3/3)/2}]$ determined by Eq. (2.19), the corresponding straight line also intersects the triangle; the realizability conditions (2.6) are invalid below this straight line. Hence, none of the models (except for the GL model for which the weak inequality $C_2 \geqslant 2C_3/3$ turns into an equality) can be recognized as adequate. In particular, these models are inapplicable for calculating strongly anisotropic flows with large negative values of the parameter B_3 and, correspondingly, a positive value of the component b_{33} (high intensity of turbulent fluctuations along axis 3).

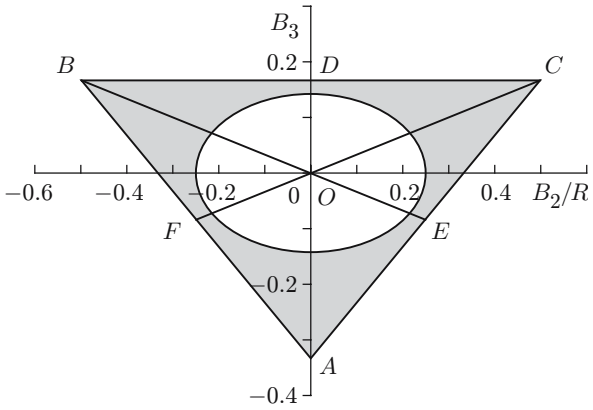

Fig. 3

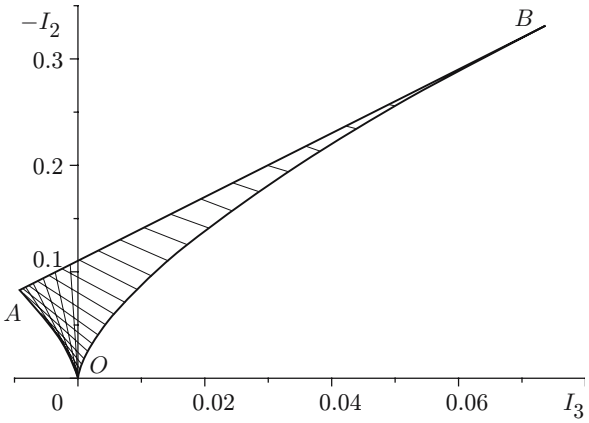

Fig. 4

Fig. 3. "Region of adequacy" of the LRR model in calculating irrotational three-dimensional distortion.

Fig. 4. Lumley triangle with the family of isolines of B_3 ($-1/3 \leqslant B_3 \leqslant 0$).

Similar calculations were performed for the second type of flows: irrotational three-dimensional distortion. In this case, the constraint is determined by inequality (1.3), and the region of the physical range of parameters where this constraint is violated is even greater than that for elliptical flows. Figure 3 shows the configuration of this region for the LRR model (hatched zone of the triangle ABC).

3. Invariant Presentation of Results. The results obtained above, in particular, constraints (2.6) on the values of the components of the anisotropy tensor b can be presented in invariant form. For this purpose, instead of the parameters $\{B_i\}$, we use the second invariant I_2 and the third invariant I_3 of this tensor (the first invariant, the convolution b_{ii}, vanishes by definition):

$$I_2 = -\{b^2\}/2, \qquad I_3 = \{b^3\}/3.$$

Figure 4 shows the so-called Lumley triangle [region of the plane (I_3, I_2)] corresponding to physically admissible values of these invariants. The Lumley triangle can be considered as one of the forms of presentation of the usual realizability conditions (2). Here the points $O(0, 0)$, $A(-1/108, 1/12)$, and $B(2/27, 1/3)$ correspond to isotropic, isotropic two-dimensional, and one-dimensional turbulence. The line AB defined by the formula

$$-I_2 = 1/9 + 3I_3$$

corresponds to two-dimensional turbulence. The side boundaries are defined by the equation

$$-I_2 = 3(I_3/2)^{2/3} \tag{3.1}$$

and correspond to axisymmetric turbulence.

The expressions that establish the relation between the invariants I_2 and I_3 and the parameters $\{B_i\}$ have the form [12]

$$-2I_2 = B_1^2 + 2B_2^2/R^2 + 6B_3^2, \qquad I_3 = B_3(B_1^2 + 2B_2^2/R^2 - 2B_3^2). \tag{3.2}$$

Let us analyze these expressions in more detail. First we consider the parameter B_3, for which Eq. (3.2) yields the following relation:

$$I_3 = -2B_3(I_2 + 4B_3^2). \tag{3.3}$$

Relation (3.3) can be presented as a cubic equation

$$B_3^3 - (-I_2/4)B_3 + I_3/8 = 0,$$

which allows finding the values of the parameter B_3 from given values of the invariants. This equation is the equation of the so-called incomplete ($x^3 + px + q = 0$) form ($p = I_2/4$ and $q = I_3/8$). The character of its solution is determined by the sign of the expression $Q \equiv (p/3)^3 + (q/2)^2$.

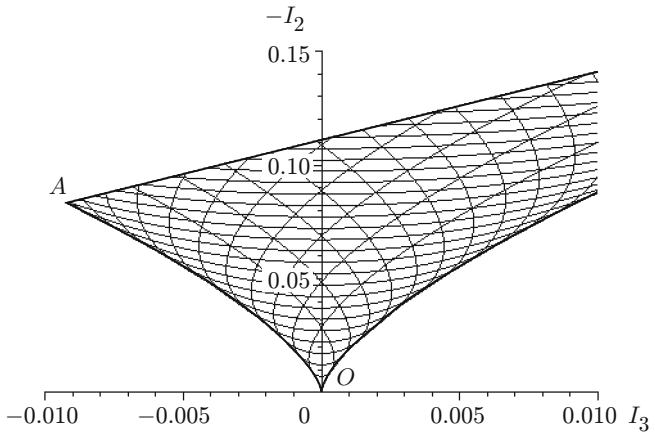

Fig. 5

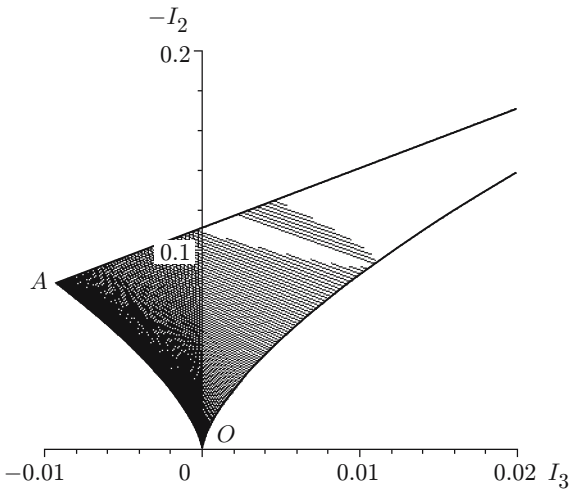

Fig. 6

Fig. 5. Fragment of a physically admissible region of parameters with a grid of isolines of B_2 ($B_1 = 0$).

Fig. 6. "Region of adequacy" of the SSG model in the plane of the invariants I_2 and I_3 ($R = 0.2$ and $B_1 = 0$).

Expressing Q through the invariants as

$$Q = ((I_3/2)^2 + (I_2/3)^3)/64$$

and taking into account Eq. (3.1) for the boundary of the admissible region of the plane (I_3, I_2), we can readily conclude that $Q \leqslant 0$. Hence, Eq. (3.3) has three real roots (there are two roots only in the limiting case $-I_2 = 3(I_3/2)^{2/3}$ corresponding to axisymmetric turbulence). In other words, three values of the parameter B_3 correspond to each point in the admissible region in the plane (I_3, I_2). This result admits clear geometric interpretation (see Fig. 4). For a given value of B_3, Eq. (3.3) defines a straight line in the plane (I_3, I_2). For all values of B_3 within the interval $[-1/3, 1/6]$, the corresponding straight line intersects the domain of the admissible region. The segment where this intersection occurs can be considered as a corresponding isoline of B_3. We can easily verify that the family of these isolines goes around the admissible region three times, so we can speak about three "sheets" or copies of this region covered by the isolines of B_3. Figure 4 shows the first "one and a half sheets" corresponding to the values of B_3 within the interval $[-1/3, 0]$. Note that the isoline $B_3 = -1/3$ degenerates into a point, and the value $B_3 = 1/6$ [as it follows from (3.3)] corresponds to the isoline coinciding with the upper boundary $-I_2 = 1/9 + 3I_3$ of the domain.

The side boundaries $-I_2 = 3(I_3/2)^{2/3}$ of the region coincide with the envelope of the family of the straight lines (3.3). Hence, the above-made conclusion on the "three-sheet" correspondence can be supplemented by the following geometric constructions. From each point admissible for the region, we can draw three tangent lines to the side boundaries $-I_2 = 3(I_3/2)^{2/3}$. In the general case, each of these straight lines corresponds to three different values of B_3. These values [which are readily identified with the use of construction or Eq. (3.3)] correspond to the point chosen in the plane (I_3, I_2).

The procedure of identification of the isolines of B_2 and B_1 is more complicated. In particular, a simple analytical calculation of the isolines of B_2 can only be possible for $B_1 = 0$. The corresponding family of isolines is plotted in Fig. 5. As for the parameter B_3, here we have a triple correspondence between the values of $|B_2|$ and a given point in the region; the isoline $B_2 = 0$ corresponds to the side boundaries of the region.

For $B_1 \neq 0$, the family of the isolines of B_2 is calculated numerically on the basis of Eqs. (3.2): for a fixed value of the parameter B_1, these equations define the corresponding isoline for each value of B_2 in parametric form. The quantity B_3 is used as a parameter; the range of possible values of this parameter is determined by relations (2.8) and (2.10).

Using the auxiliary results obtained, we can easily present and analyze the character of constraints (2.6) in the plane (I_3, I_2) in "invariant" form. For certainty, we confine ourselves to considering a set of constants corresponding to the SSG model (the results for other models are similar).

The calculation is performed in a manner similar to that performed in constructing the isolines. In addition to the standard conditions (2.8) and (2.10), however, we take into account constraint (2.6). The "forbidden" zones inside the main region (I_3, I_2) are easily identified for each model considered. These zones are sets of those isolines or their segments for which condition (2.6) is violated.

The results calculated for $R = 0.2$ and $B_1 = 0$ are plotted in Fig. 6; the hatched region shows the part of the domain where the main inequality (2.6) is not violated.

It should be noted that these conclusions are only alternative presentations of the results obtained above, which are illustrated, in particular, in Fig. 2.

Conclusions. The study performed shows that many approximations of the pressure–strain rate correlations used for closing the transport equations for the Reynolds stresses cannot be considered as sufficiently accurate ones. In particular, they cannot be used to calculate flows with an arbitrary degree of anisotropy. The results of attempts to expand the area of applicability of the models by varying the values of the constants or replacing them by certain functions of flow parameters (including investigations with allowance for the above-derived constraints on the values of the constants and calculation of the "regions of adequacy") usually indicate the principal drawbacks of the models: turbulence is nonlocal to a greater degree than that assumed in these models. For this reason, the set of fields for which differential equations are derived has to be increased in the general case. This conclusion, however, does not reduce the significance of these models in engineering calculations, in particular, in calculating the steady-state parameters.

REFERENCES

1. C. G. Speziale, S. Sarkar, and T. B. Gatski, "Modeling the pressure-strain correlation of turbulence: an invariant dynamical systems approach," *J. Fluid Mech.*, **227**, 245–272 (1991).
2. B. E. Launder, G. Reece, and W. Rodi, "Progress in the development of a Reynolds stress turbulence closure," *J. Fluid Mech.*, **68**, 537–566 (1975).
3. M. M. Gibson and B. E. Launder, "Ground effects on pressure fluctuations in the atmospheric boundary layer," *J. Fluid Mech.*, **86**, 491–511 (1978).
4. D. B. Taulbee, "An improved algebraic stress model and corresponding nonlinear stress model," *Phys. Fluids, Ser. A*, **4**, 2555–2561 (1992).
5. J. Lumley, "Second-order modeling of turbulent flows," in: W. Kollmann (ed.), *Prediction Methods for Turbulent Flows*, Hemisphere, Washington (1980).
6. S. R. Bogdanov and S. I. Sobolev, "On the problem of modeling of the pressure–strain rate correlations in the turbulence theory," *Izv. Ross. Akad. Nauk, Mekh. Zhidk. Gaza*, No. 2, 42–46 (1992).
7. S. R. Bogdanov and T. J. Jongen, "Constraints for the pressure-strain correlation tensor derived from spectral representation," in: *Abstr. of the 6th Fluid Mech. Conf.* (EUROMECH) (Stockholm, Sweden, June 26–30, 2006), Vol. 2, Roy. Inst. of Technol., Stockholm (2006), p. 224.
8. A. S. Monin and A. M. Yaglom, *Statistische Hydromechanik.* 1. *Mechanik der Turbulenz*, Verlag–Nauka, Moskau (1965).
9. V. I. Smirnov, *Course of Higher Mathematics* [in Russian], Vol. 3, Part 1, Nauka, Moscow (1974).
10. T. Jongen and T. B. Gatski, "A new approach characterizing the equilibrium states of the Reynolds stress anisotropy in homogeneous turbulence," *Theoret. Comput. Fluid Dyn.*, No. 11, 31–47 (1998).
11. S. C. Kassinos and W. C. Reynolds, "A particle representation model for the deformation of homogeneous turbulence," *Annu. Res. Briefs*, Center Turbulence Res. (1996), pp. 31–51.
12. T. Jongen and T. B. Gatski, "A unified analysis of planar homogeneous turbulence using single-point closure equations," *J. Fluid Mech.*, **399**, 117–150 (1999).